Available online at www.sciencedirect.com
SCIENCE DIRECT
Journal of Sound and Vibration 293 (2006) 522–534
JOURNAL OF SOUND AND VIBRATION
www.elsevier.com/locate/jsvi

A comprehensive track model for the improvement of corrugation models

J. Gómez*, E.G. Vadillo, J. Santamaría

Department of Mechanical Engineering (Higher School of Engineering), University of the Basque Country, Alameda de Urquijo s/n, 48013-Bilbao, Spain

Accepted 26 August 2005
Available online 10 March 2006

Abstract

This paper presents a detailed model of the railway track based on wave propagation, suitable for corrugation studies. The model analyses both the vertical and the transverse dynamics of the track. Using the finite strip method (FSM), only the cross-section of the rail must be meshed, and thus it is not necessary to discretise a whole span in 3D. This model takes into account the discrete nature of the support, introducing concepts pertaining to the theory of periodic structures in the formulation. Wave superposition is enriched taking into account the contribution of residual vectors. In this way, the model obtains accurate results when a finite section of railway track is considered. Results for the infinite track have been compared against those presented by Gry and Müller. Aside from the improvements provided by the model presented in this paper, which Gry's and Müller's models do not contemplate, the results arising from the comparison prove satisfactory. Finally, the calculated receptances are compared against the experimental values obtained by the authors, demonstrating a fair degree of adequacy. Finally, these receptances are used within a linear model of corrugation developed by the authors.

1. Introduction

The track model presented here was first developed to study the process of periodic wear observed on the rail surface due to regular traffic, identified as railway track corrugation. This wear, a well known fact on most railway systems [1], mainly on subways, increases noise levels and could even cause damage to some components of the track. Regular treatment, consisting of periodic grinding of the rails, merely removes the symptoms and leads to high costs. For this reason, the problem must be investigated analysing the appearance and development of the undulatory wear process by means of a model, which includes the main system elements, so that a basic solution can be found from optimising track and vehicle parameters.

A number of models has been presented in recent years in an attempt to explain this phenomenon. The track model used in each is a key factor to determine the mechanism to set the corrugation wavelength.

*Corresponding author. Tel.: +34 94 601 4223; fax: +34 94 601 4215.
E-mail address: ernesto.qarciavadillo@ehu.es (J. Gómez).

0022-460X/$ - see front matter © 2006 Published by Elsevier Ltd.
doi:10.1016/j.jsv.2005.08.064

Nomenclature

$\{a_n(x,t)\}$	generalised displacements ($n=1,\ldots,N$)
$\mathbf{f}_n$	forces acting on the end sections
$\mathbf{F}$	vector N related to forces in the cross-section of rail
G function	corrugation growth indicator
$\mathbf{H}$	impedance matrix of the support
k_i	wavenumber
L	rail section length
$\mathbf{M}$	matrix $N\times N$ related to inertia properties of rail
N_{wf}	number of wave functions used for calculating receptances of rail
$\mathbf{R}_t$	vector representing the part of the load not contained in the waves held back
$\mathbf{R}_0$	projection of the force applied to a point on rail over the space of the waves taken for the static case
$\mathbf{R}_s$	projection of the force applied over the space of the waves taken for the dynamic case
t	time
$\mathbf{T}$	transfer matrix
$\{\mathbf{u}^n\}$	section functions ($n=1,\ldots,N$)
$\mathbf{U}$	state vector of span
$\mathbf{V}$	vector N related to longitudinal forces in rail
(x,y,z) (m)	rail displacements
$\mathbf{Z}$	impedance matrix
ω (rad/s)	rotational frequency, $\omega=2\pi f$
λ,μ	Lamé coefficients of rail
λ_i	characteristic wavenumber
ρ	density of rail
$\boldsymbol{\sigma}$	stress tensor
$\boldsymbol{\varepsilon}$	strain tensor
$\boldsymbol{\varphi}_{\mathrm{i}}^{\mathrm{R}}$	characteristic wave travelling towards the right
$\boldsymbol{\varphi}_{\mathrm{i}}^{\mathrm{L}}$	characteristic wave travelling towards the left
$\boldsymbol{\Phi}_{\mathrm{wfstc}}$	matrix of wave functions for the static case
$\boldsymbol{\Phi}_{\mathrm{wfdyn}}$	matrix of wave functions for the dynamic case
$\boldsymbol{\Psi}_i$	characteristic wave shapes
$\boldsymbol{\Phi}_{\mathrm{i}}$	wave shape
$\boldsymbol{\Pi}$	vector N related to force produced by support

Owing to the importance of track transfer functions in the prediction of frequencies at which corrugation is more likely to appear, an improvement in the calculation of receptances or accelerances for both vertical and lateral component allows to obtain these frequencies more accurately. Furthermore, an inadequate agreement between experimental and calculated receptances could lead not only to a slight shift in frequency of corrugation but also to an incorrect prediction of the probability of corrugation development.

One of the earliest comprehensive examinations of the dynamic behaviour of the track, much used in subsequent corrugation models as for example in articles by Tassilly and Vincent [2,3], is provided by Grassie [4]. However, as the authors have shown, the results obtained with a rail model using a Timoshenko beam do not represent accurately enough the results observed in the experimental data for the lateral component, even in the medium frequency range.

In order to include higher modes, Ripke models the rail head and foot separately as two Timoshenko beams with an elastic coupling between them. In corrugation work by Ripke and Knothe [5], Hempelmann [6] and Müller [7], this track model is used to characterise undulatory wear. This model, which examines vertical and lateral behaviour of the track considers discrete support, and the rail is meshed with finite elements over the entire length of the span.

Extending the finite element method has led to development of models, which improve the treatment of the foot and the web, and so better results are obtained for modes with large cross-section deformations [8,9]. Thompson [10] added a model of these characteristics to the track model. The track model is considered to have continuous support, and so in accordance with the theory of periodic structures, it is only necessary to discretise a small section of rail (1 cm).

In recent years, Wu and Thompson [11,12] examined vertical and lateral rail dynamics separately by using beams, and submitted further papers on the influence of a number of wheel sets on the track [13,14].

Gavric [15] and Gry [16,17] have calculated the frequency–wavenumber relation, and hence deformation of the rail cross-section by using the finite strip method (FSM). When this method is used, it is only necessary to

discretise the rail section in two dimensions instead of producing a 3-D mesh for a finite section. Moreover, the track model proposed by Gry [16] considers discrete support using the theory of periodic structures.

In accordance with the work of these two authors and Mead [18], a track model based on FSM and the theory of periodic structures is presented. The track model consists of an infinite rail whose section is discretised accurately using linear or second order quadrilateral elements. The discrete nature of the support is considered by the model. The dynamic characteristics of the infinite track, expressed through receptances, are obtained from superposition of the waves travelling along the infinite rail with support. This model has been implemented in MATLAB [19].

The precision of the model improves when increasing the number of waves taken into account. Nevertheless, due to the nature of the structure itself, increasing the number of waves would require more precision when calculating the corresponding eigenvalues.

In the numerical formulation carried out by Gry, which uses the transfer matrix and its inverse, certain error in the calculation of eigenvectors is assumed, even, as in the case of Gry, when quite a low number of waves was considered. However, since there is a great variation in the results as a function of wavenumber, as observed by the authors, a large number of waves have been incorporated in the model presented in the paper.

Since MATLAB's precision is insufficient to cope with all the relevant waves, the eigenvalue calculation is carried out using the variable precision arithmetic in the MAPLE programme [20]. At the same time, a finite section of track has been studied to compare results with those obtained by a commercial finite element package.

Thanks to this comparison, the method to improve the results obtained by modal frequency response analysis based on residual vectors, which is implemented in some finite element commercial packages (such as MSC/NASTRAN [21]), has been extended to cover infinite structures, and implemented in the model presented in this paper.

2. Railway track model description

2.1. Introduction

The FSM reduces the computational effort inherent to the finite element method, retaining versatility to a large extent. Whereas polynomial functions are used in the finite element method for multidirectional displacements, the FSM uses polynomial functions in given directions (the cross-section plane for the rail) and continuous differentiable series in other directions (the direction along which the rail extends infinitely in this case). These last series must comply with the boundary conditions on the end sections of the structure [22]. The general form of the displacement function is thus expressed as a product of polynomials and series.

In the case of rails, the displacement at a point (x, y, z) over a time interval t may be given using N arbitrary section functions or modes, $\mathbf{u}^n(y,z) = (\mathbf{u}_x^n(y,z), \mathbf{u}_y^n(y,z), \mathbf{u}_z^n(y,z))^{\mathrm{T}}$, as

$$\mathbf{u}(x,y,z,t) = \sum_{n=1}^{N} a_n(x,t)\mathbf{u}^n(y,z), \tag{1}$$

where $a_n(x,t)$ are the so-called generalised displacements depending on axial coordinates and time.

Section functions taking part in the development are, in principle, arbitrary. The rail is considered as an infinite and homogeneous medium with Lamé coefficients, λ and μ and density ρ. Once the displacement field has been defined using section functions and generalised displacements, strains and stresses can be found. By applying the virtual work principle to a length of rail L, the equation describing the rail dynamics is calculated:

$$\mathbf{F}(x,t) - \mathbf{V}'(x,t) = -\mathbf{M}\ddot{\mathbf{a}}(x,t). \tag{2}$$

With boundary conditions:

$$\mathbf{V}(0^+,t) + \mathbf{\Pi}(0,t) = \mathbf{V}(0^-,t), \tag{3}$$

$$\mathbf{V}(L^-,t) + \mathbf{\Pi}(L,t) = \mathbf{V}(L^+,t), \tag{4}$$

where $\mathbf{a}(x,t)$ is an N order vector of components $a_n(x,t)$ and $\mathbf{F}(z,t)$, $\mathbf{V}(z,t)$, $\mathbf{\Pi}(0,t)$ and $\mathbf{\Pi}(L,t)$ are N order vectors with their Nth components given by the expressions

$$F^n(x,t) = \int_{S(x)} (\sigma_{yy}\varepsilon^n_{yy} + 2\sigma_{yz}\varepsilon^n_{yz} + \sigma_{zz}\varepsilon^n_{zz} + \sigma_{yx}\partial_y u^n_x + \sigma_{zx}\partial_z u^n_x)\,\mathrm{d}S, \tag{5}$$

$$V^n(x,t) = \int_{s(x)} \boldsymbol{\sigma}_x \cdot \mathbf{u}^n\,\mathrm{d}S, \tag{6}$$

$$\Pi^n(0,t) = \int_{\gamma_0} \mathbf{f}_0 \cdot \mathbf{u}^n\,\mathrm{d}S, \tag{7}$$

$$\Pi^n(L,t) = \int_{\gamma_1} \mathbf{f}_1 \cdot \mathbf{u}^n\,\mathrm{d}S, \tag{8}$$

where $S(x)$ is the cross-section at abscissa x; $\boldsymbol{\sigma}_x = (\sigma_{yx}, \sigma_{zx}, \sigma_{zy})$ the stress vector in a direction parallel to axis x; $\mathbf{f}_0(x_\gamma, y_\gamma)$ and $\mathbf{f}_1(x_\gamma, y_\gamma)$ the forces exerted by supports on contact lines γ_0 and γ_1, respectively; and terms $\varepsilon^n_{yy}, \varepsilon^n_{yz}$ y ε^n_{zz} represent strains on section associated with function $\mathbf{u}^n$.

Using the Lamé stress–strain relationship, $\mathbf{F}(x,t)$ and $\mathbf{V}(x,t)$ can be expressed as follows:

$$\mathbf{F}(x,t) = \mathbf{A}\mathbf{a}(x,t) + \mathbf{B}\mathbf{a}'(x,t), \tag{9}$$

$$\mathbf{V}(x,t) = \mathbf{C}\mathbf{a}(x,t) + \mathbf{D}\mathbf{a}'(x,t) \tag{10}$$

each of the elements in the $\mathbf{A}$, $\mathbf{B}$, $\mathbf{C}$, $\mathbf{D}$ and $\mathbf{M}$ $N \times N$ order matrices consists of integrals whose integrands depend on λ, μ, and ρ, the strain tensor elements and the displacement components.

Substituting $\mathbf{F}(x,t)$ and $\mathbf{V}(x,t)$ into Eq. (2) and applying the Fourier time transform to all variables, the following equation is obtained:

$$\mathbf{D}\mathbf{a}''(x) + (\mathbf{C} - \mathbf{B})\mathbf{a}'(x) + (\omega^2\mathbf{M} - \mathbf{A})\mathbf{a}(x) = \mathbf{0}, \tag{11}$$

where the convention of designating variable Fourier transforms with the variable name itself has been applied, except that variable t has been eliminated.

Matrices $\mathbf{D}$ and $\mathbf{G} = (\omega^2\mathbf{M} - \mathbf{A})$ are symmetrical, whereas $\mathbf{E} = \mathbf{C} - \mathbf{B}$ is anti-symmetrical, and this characteristic shows that there are two opposite directions of wave propagation.

To solve the differential equation system (11), solutions of the type $\mathrm{e}^{kx}\mathbf{\Phi}$ are tested, the system being thus turned into a generalised problem of eigenvalues for complex scalar k, and $\mathbf{\Phi}$, N order vector defining the wave shape:

$$(\mathbf{D}k^2 + \mathbf{E}k + \mathbf{G})\mathbf{\Phi} = 0. \tag{12}$$

The $2N$ solutions of the system of equations constitute a set of free waves for the rail, i.e., they represent the waves transmitted along the infinite rail without support. Once the complete set of the $2N$ free waves of the system for this approximation has been obtained, Fourier transforms of the N generalised displacements for each x, $\mathbf{a}(x)$ may be expressed in the $2N$-dimensional wave vector space, as

$$\mathbf{a}(x) = \sum_{j=1}^{2N} \alpha_j \mathrm{e}^{k_j x}\mathbf{\Phi}_j. \tag{13}$$

2.2. Introducing the support to the model

So far, a rail section of arbitrary length L, regardless of the support, has been analysed. Including the support in the model requires a thorough analysis of the junction of two rail sections in the presence of the support; but, above all, the discrete nature of the support along the rail requires the inclusion of basic concepts of the periodic structure theory in the formulation.

First of all, a state vector $\mathbf{U}$ for each span is defined; its components being the displacements at both ends of the span. For span k, L being the length of the span, the state vector using generalised displacements is

$$\mathbf{U}_k = \begin{bmatrix} \mathbf{a}_k(0) \\ \mathbf{a}_k(L) \end{bmatrix}. \tag{14}$$

On the basis of the conventional linear and perfect periodicity hypotheses, a transfer matrix $\mathbf{T}$ between consecutive spans can be established, so that the wave propagation equation can be written as

$$\mathbf{U}_{k+1} = \mathbf{T}\mathbf{U}_k. \tag{15}$$

To enable us to find the transfer matrix and to know how waves travel from span to span, the relationship within a span k of the generalised forces acting on the end sections, $-\mathbf{f}_{n-1}$ and $\mathbf{f}_n$, with displacements of nodes of the same sections $\mathbf{u}_{k-1}$ and $\mathbf{u}_k$, is first established. This defines the impedance matrix $\mathbf{Z}$. This matrix can be calculated from Eq. (10) expressing generalised displacements and their derivatives as superposition of free waves.

At the junction of spans, k and k+1, there must be compliance with generalised displacement continuity. Similarly, the balance between all forces involved must be verified, and this includes the response of support, $\mathbf{\Pi}$.

From this, the span and support impedance matrix being known, the transfer matrix $\mathbf{T}$ is obtained:

$$\mathbf{T} = \begin{bmatrix} \mathbf{0} & \mathbf{I} \\ -\mathbf{Z}_{12}^{-1}\mathbf{Z}_{21} & -\mathbf{Z}_{12}^{-1}(\mathbf{Z}_{11} + \mathbf{Z}_{22} + \mathbf{H}) \end{bmatrix}, \tag{16}$$

where $\mathbf{Z}_{11}, \mathbf{Z}_{12}, \mathbf{Z}_{21}$ and $\mathbf{Z}_{22}$ are $N \times N$ submatrices constituting the impedance matrix elements; $\mathbf{H}$ the impedance matrix of the support, which relates the force exerted by the support, $\mathbf{\Pi}(L)$, with the generalised displacements at the junction $\mathbf{a}(L)$; and $\mathbf{I}$ the $N \times N$ order identity matrix.

2.3. Analysis of the transfer matrix

From the definition of the transfer matrix in Eq. (15), it may be deduced that diagonalisation of $\mathbf{T}$ permits uncoupling the problem, finding pure waves transmitted from one span to another. These free waves related to the rail resting on the supports, represented by the pair $(\lambda_i, \mathbf{\Psi}_i)$, are designated as characteristic waves of the track. Vector $\mathbf{\Psi}_i$ defines the shape of the characteristic wave i of the section, whereas the argument of complex eigenvalue λ_i defines the wavelength, and its module, the attenuation along the axis x. On a periodic structure, it can be shown that these eigenvalues appear on inverse pairs $(\lambda_i, 1/\lambda_i)$, corresponding, respectively, to waves travelling towards the left and waves travelling towards the right.

If state vectors $\mathbf{U}_k$ and $\mathbf{U}_{k+1}$ are expanded on the eigenvectors basis $\{\mathbf{\Psi}_i\}$, taking separately into account waves travelling towards the right, $\boldsymbol{\varphi}_i^R$ and waves travelling towards the left, $\boldsymbol{\varphi}_i^L$, the expressions for generalised displacements obtained for the spans k and $k+1$ are as follows:

$$\mathbf{a}_k(x) = \sum_{i=1}^{N} (a_i \boldsymbol{\varphi}_i^R(x) + b_i \boldsymbol{\varphi}_i^L(x)),$$

$$\mathbf{a}_{k+1}(x) = \sum_{i=1}^{N} (\lambda_i a_i \boldsymbol{\varphi}_i^R(x) + (1/\lambda_i) b_i \boldsymbol{\varphi}_i^L(x)). \tag{17}$$

These specific equations, to find generalised displacements at junctions ($x = 0$ and L), lead to similar expressions for the generalised forces by using the span impedance matrix concept.

2.4. Support model

The support model to obtain the support impedance matrix $\mathbf{H}$, appearing in the transfer matrix, consists of half a sleeper considered as a mass with six degrees-of-freedom coupled to the ground through a ballast-like element, providing stiffness and hysteretic damping for each of the six degrees-of-freedom, three translations

and three rotations. The rail is fastened to the sleeper through three damping springs simulating the pad. These elements contribute stiffness and hysteretic damping and are located at three different nodes (two near the end and one in the middle) on the rail foot, so as to allow the rail to roll on the pad. All these elements have all three translation degrees-of-freedom.

The impedance matrix of the support is calculated establishing the sleeper balance under the action of the ballast and a force exerted on the points shared by the rail through the elements constituting the pad.

2.5. Calculation of receptances

The procedure to calculate the track transfer function depends on the specific point on the rail. Two distinct analyses are: studying the behaviour of the rail at a point inside the span, say at midspan, or at a point on the rail over the sleeper, i.e., just at the junction of two spans. In both cases, compliance with two conditions for the section containing the point is required, and they are the continuity of displacements and the balance of forces.

3. Computation problems

One of the problem areas in the above method for track behaviour analysis is the large number of degrees-of-freedom required to calculate characteristic waves for each frequency, if interpolation functions derived from finite element analysis are used as cross-section functions in Eq. (1). Nevertheless, this calculation will only be required once because, as Gry [16] has pointed out, and the authors of this paper have proved, few wave shapes corresponding to calculated free waves for a low frequency, say 100 Hz, used as section functions, reproduce accurately enough the free waves of the system at any frequency within the range of the study for the presented model, about 2000 Hz.

For free wave calculation at a frequency of 100 Hz, interpolation functions relative to the four- or eight-node quadrilateral element are used as cross-section functions.

On the basis of the $2N$ rail free waves obtained with this discretisation, the number of wave functions $2N_{\mathrm{wf}}$ required to obtain accurate results is investigated. On rails studied by the authors, the first six free waves include the classical deformation modes: elongation, vertical and lateral bending, both propagation and decaying, and torsional waves.

Beyond $N_{\mathrm{wf}} = 6$, waves show the increasingly significant bending of the web, and the corresponding sections show increasing distortion. The number N_{wf} of waves ($2N_{\mathrm{wf}}$ section functions in the model) selected to describe the behaviour of the rail must be such that a compromise solution between accuracy and costs related to computation difficulties is obtained.

Computation difficulties arise as a result of poor conditioning of the transfer matrix $\mathbf{T}$. Sources of this poor conditioning are: on the one hand, the presence of waves travelling towards the left and the right, bringing about inverse exponential terms of the form e^{kL} and e^{-kL}; and on the other hand, the increasing value of the real parts of the exponents of said expressions with increasing number of waves N_{wf}, thus taking into account waves with increased attenuation.

Moreover, since the exponential terms depend on the length of the span, the longer the span of the rail considered, the worse the conditioning.

This poor conditioning of the matrix $\mathbf{T}$ is an unavoidable characteristic; characteristic waves have associated eigenvalues with modulus close to one, and eigenvalues, which, even with low N_{wf}, have a modulus of 10^{18} or 10^{-18}. This track model has been implemented using software MATLAB 6 [19], but 15-digit default precision implemented in MATLAB 6 is not sufficient. The authors of this paper have found that the application of the LinearAlgebra module of version MAPLE 7 [20] to solve the problem of matrix $\mathbf{T}$ eigenvalues and eigenvectors gives very accurate results, and with less computation costs than with other modules and previous version of MAPLE (version 4 of MAPLE V [23]).

The authors have carried out an analysis on various tracks, consisting of different types of elements such as UIC54 rail and UIC60 rail; monobloc and double block sleepers; ballast and concrete slab. This study has proved that considering only the 11 least decaying waves (22 section functions), the model provides accurate results for the receptances on the lateral component, provided that eigenvalues and eigenvectors of $\mathbf{T}$ are

calculated with 50-digit arithmetic. For the vertical case, satisfactory results are obtained using the six least decaying waves, classical beam waves, with 30-digit arithmetic.

4. Comparison with the results of a commercial programme (NASTRAN) for a finite section

The accuracy of the results obtained using the model based on Gry [16,17], utilising the FSM in conjunction with the periodic theory was estimated by comparing the results obtained with those obtained by the commercial finite elements programme MSC/NASTRAN [21] for the same section of track, which can have an arbitrary number of identical spans connected by a supporting device.

This intermediate stage allows us to observe the considerable importance of incorporating residual vectors in calculations of the transfer function by modal superposition. The residual vectors indirectly introduce the contribution of non-participating modes in superposition. The importance of this may be appreciated by the frequencies at which anti-resonances are produced in the transfer function, depending on whether the residual vectors are incorporated or not. This may be seen in Fig. 1, showing the receptances for a beam of dimensions similar to that of the rail.

Besides, regarding computing time, analysing with NASTRAN [21] a section of 150 spans of track (minimum number of spans needed for accurate results in lateral component), with the rail cross-section meshed with 175 nodes, as in the case of Gry, overflows the memory of a Pentium IV computer. Therefore, a comparison of computing times between a 3-D solid model and the model developed by the authors should be made for a more coarse mesh. If the cross-section is meshed with 32 nodes and is used along 30 spans, the programme developed in MATLAB with the FSM and taking into account the 11 least decaying waves requires a computing time 10 times less than that required for using 3-D solid elements. In fact, the typical calculating time required for using the model developed by the authors for a frequency range of [100–3000] Hz and taking into account the 11 least decaying waves is less than 20 min.

5. Method to improve wave superposition

Therefore, to increase the accuracy of the track model, a method has been used to improve the results of wave superposition, similar to the technique used in mode superposition with the modal truncation augmentation method [24].

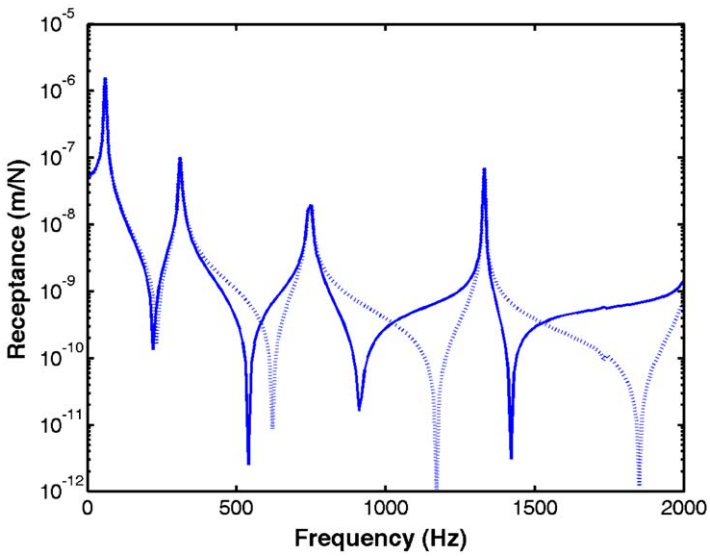

Fig. 1. Receptance for a beam with dimensions similar to rail obtained in NASTRAN using residual vectors (-) and without considering residual vectors (⋯).

Here we treat separately the static, or very low frequency, case and the dynamic case. A different number of free waves may be taken in each case as section functions. It is evident that only when the number of waves used for the static case exceeds the number in the dynamic case, a non-zero number of residual vectors may be obtained; thus leading to improved wave superposition.

In accordance with a method similar to the case of the modes, and according to the Dickens algorithm [24], vector $\mathbf{R}_t$ representing the part of the load not contained in the waves retained is calculated first. In the case of the rail waves, this vector will be as follows:

$$\mathbf{R}_t = \mathbf{R}_0 - \mathbf{R}_s, \tag{18}$$

where

$$\mathbf{R}_0 = \mathbf{\Phi}_{\text{wfstc}} \mathbf{\Phi}_{\text{wfstc}}^{\text{T}} \mathbf{F}, \tag{19}$$

$$\mathbf{R}_s = \mathbf{\Phi}_{\text{wfdyn}} \mathbf{\Phi}_{\text{wfdyn}}^{\text{T}} \mathbf{F}, \tag{20}$$

where $\mathbf{R}_0$ is the projection of the force applied to a point on rail $\mathbf{F}$ over the space of the waves taken for the static case; $\mathbf{R}_s$ is the projection of the force applied $\mathbf{F}$ over the space of the waves taken for the dynamic case; $\mathbf{\Phi}_{\text{wfstc}}$ is the matrix of wave functions for the static case; and $\mathbf{\Phi}_{\text{wfdyn}}$ is the matrix of wave functions for the dynamic case.

We then calculate the displacement associated with the truncation vector $\mathbf{R}_t$, using the receptance matrix calculated for the static case. In accordance with the Rose algorithm [25], these displacement vectors are directly associated with residual vectors of wave superposition.

These residual vectors may not be linear-independent among each other and with respect to the wave shapes, and thus they must be used to find a set of combined wave shapes and linear combinations of residual vectors, which are orthogonal among each other.

In the case of the rail, only three static loads are considered on the three main axes, and so a maximum of three residual vectors will be obtained, which can be added to the waves retained.

When the new set of vectors has been obtained, the new matrices of the equation of movement for each frequency are calculated, thus obtaining the system's free waves. These new free waves are used to calculate the track receptances.

The comparison between the model presented herein and the model created in MSC/NASTRAN [21] for a track section of five spans with supports, where both include the contribution of residual vectors, is extremely satisfactory, as shown in Fig. 2.

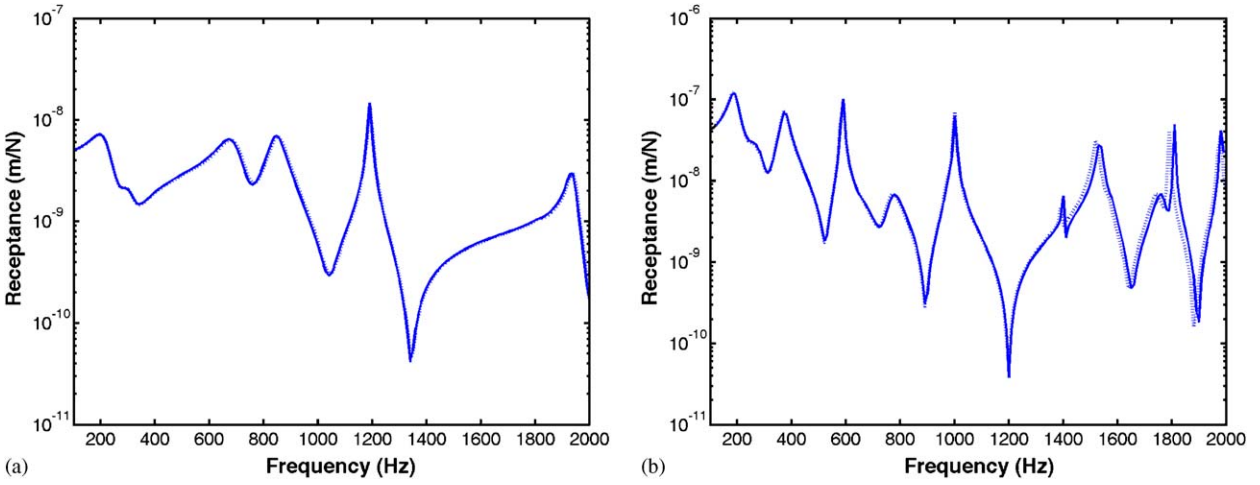

Fig. 2. Vertical (a) and lateral (b) receptance for five spans of track with support using residual vectors: (···) model in NASTRAN, (-) model with FSM.

6. Comparison with available published results

Removing the improvements introduced by the model not contemplated in the Gry [16] and Müller [7] models, the results for the track model are compared to the results obtained by these models.

Firstly, the track data used by Müller [7] are introduced in the model presented by the authors. Discretisation of the rail section (Fig. 3 (a)) and data for the support provide the receptances at midspan and over the sleeper, as shown in Fig. 4. As we may observe, this result matches with that obtained by Müller [7]. Müller's model, which considers the rail as two elastically connected infinite beams—head and foot—does not contemplate deformations on the section plane. Thus, it does without propagative waves, the influence of which on the results has been noted by the authors. It was for this reason that comparison with lateral receptance was not carried out.

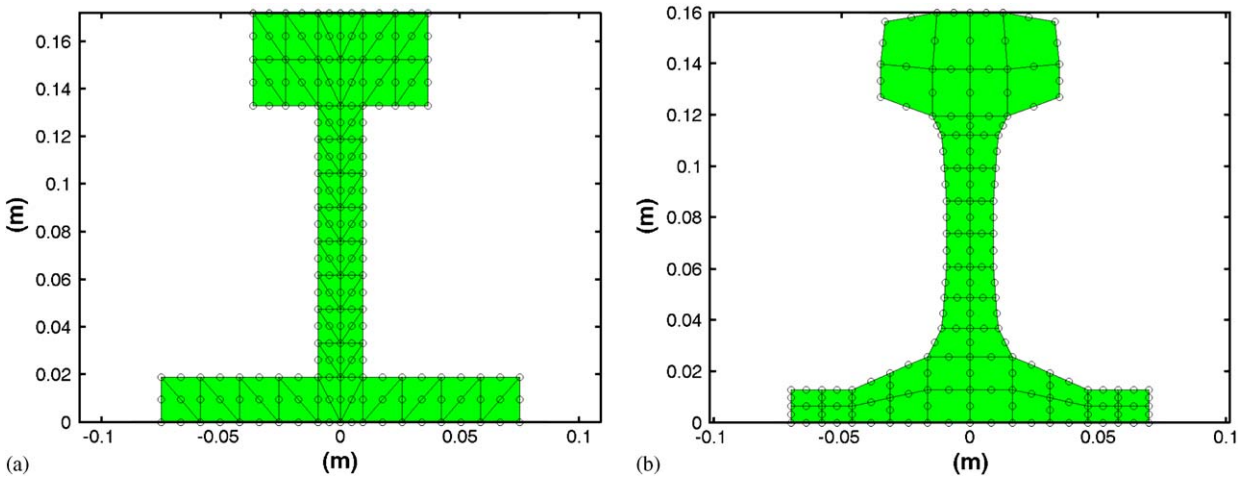

Fig. 3. Meshing for the UIC60 rail section used by Müller, consisting of 76 triangular-quadratic elements and 203 nodes (a); meshing for the UIC54 rail section used by the authors of the article, consisting of 44 quadrilateral-quadratic elements and 181 nodes (b).

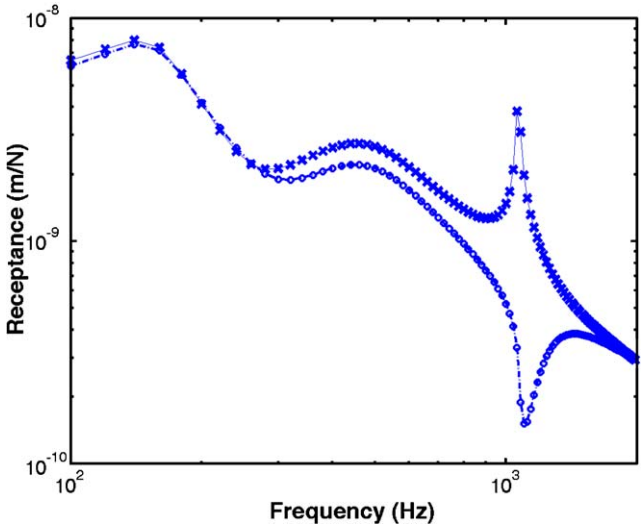

Fig. 4. Vertical receptance of the track calculated by the model presented in this article for the data used by Müller at midspan (-) and over sleeper (- - -), and comparison with Müller's model at midspan (×) and over sleeper (○).

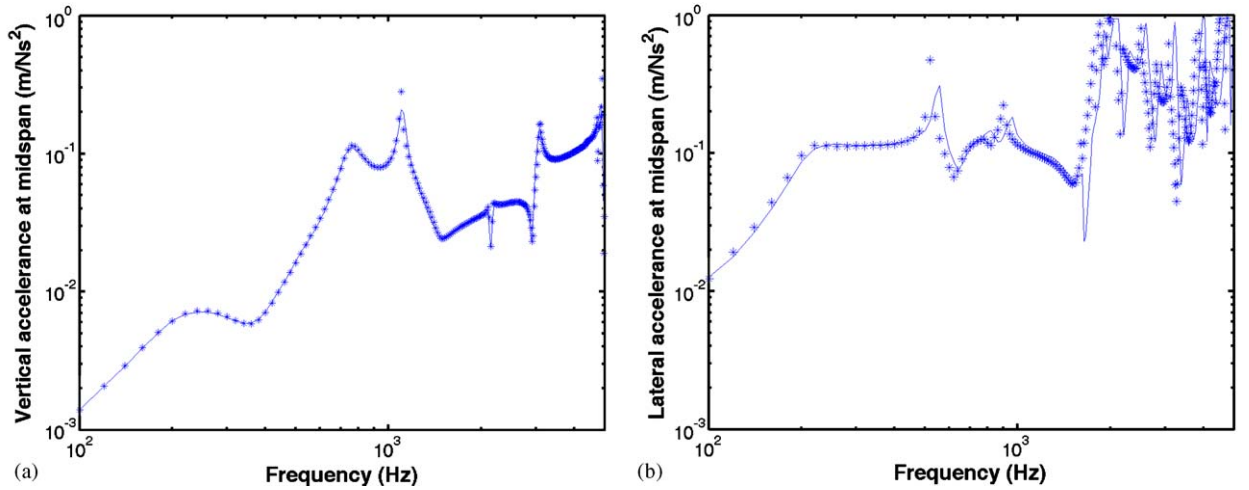

Fig. 5. Vertical (a) and lateral (b) accelerance of track at midspan obtained by the model presented in this paper for parameters shown by Gry ($\times$), and comparison with Gry's model (-).

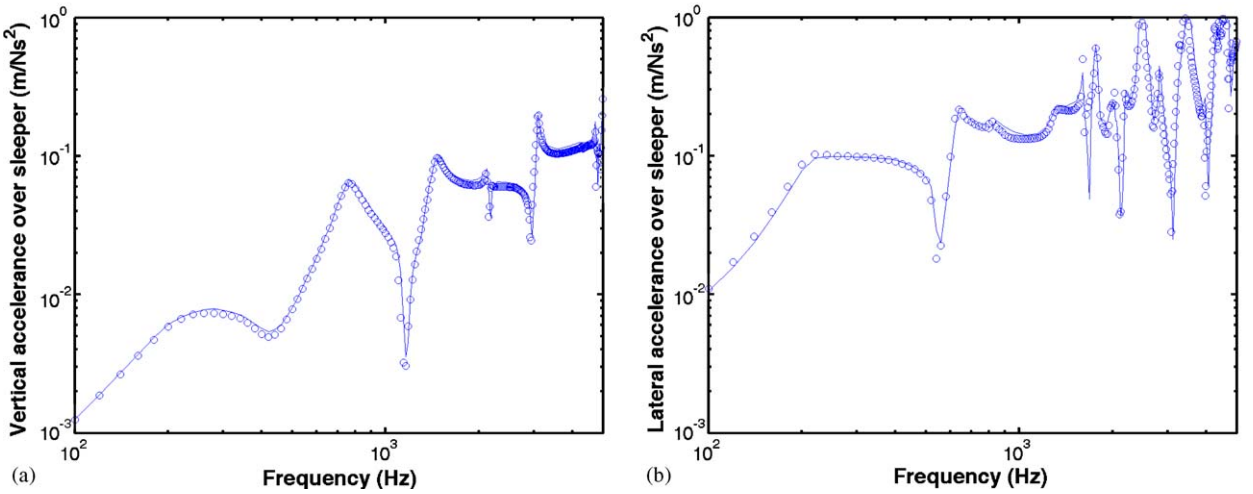

Fig. 6. Vertical (a) and lateral (b) accelerance of track over sleeper obtained by the model presented in this paper for parameters shown by Gry ($\circ$), and comparison with Gry's model (-).

Secondly, the track data presented by Gry [16] are introduced in the model. This produced the accelerances at midspan and over a sleeper, for vertical and lateral directions, shown in Fig. 5 (a, b) and Fig. 6. As may be observed, comparison of these data with the results set out by Gry [16] is very satisfactory.

7. Application of the track model to the corrugation study

By way of an example of an application, the track model presented was used to examine the corrugation process observed in a section of railway track around Bilbao [26–28]. The observed behaviour in this case differs from the modulation produced along the rail, which is observed in the main corrugation examples cited in the literature: those compiled by Grassie and Kalousek [1], and also those examined by Hempelmann and Knothe [6] and by Clark et al. [29,30].

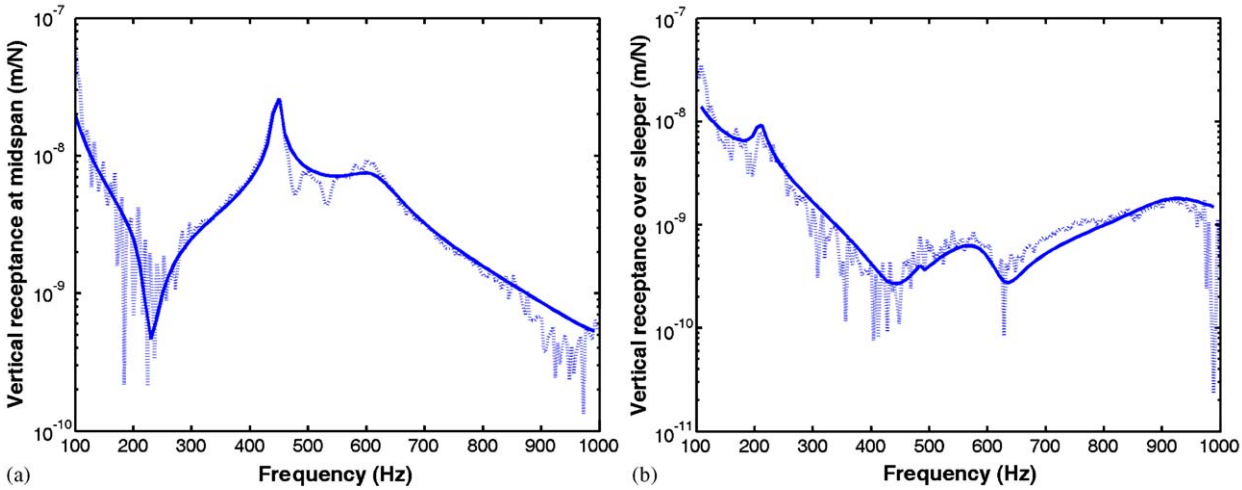

Fig. 7. Comparison between the results obtained by the model presented in this paper (-) and the experimental data (···) for vertical receptance at midspan (a) and over sleeper (b).

The receptances calculated by this track model, now including all the above-mentioned improvements, are compared to the experimental data obtained by the authors for this case. The track parameter values are given in Ref. [28]. The type of rail used in this case is UIC54, and the meshing consists of 44 elements and 181 nodes, as shown in Fig. 3 (b).

The characteristic waves required for calculation of the track's vertical receptances for both midspan and above a sleeper were obtained by taking the six waves on the free rail with least attenuation, and working with 30-digit arithmetic. For lateral receptances, the 11 waves on the free rail with least attenuation were used, and 50-digit arithmetic was employed. The comparison with the experimental results for the vertical component is shown in Fig. 7 (a, b) and, as we may observe, this is satisfactory.

It is worthy of mention that Gry's model was firstly used for studying the dynamics of the track located near Bilbao. However, the results obtained by the model developed by authors when all the above-mentioned improvements have been included are closer to the experimental results than the result obtained using Gry's model. This outcome may be due, on the one hand, to the fact that the authors' model avoids the numerical problems that appears with Gry's model. On the other hand, the use of residual vectors in the authors' model makes results more accurate, as has been shown in Section 5.

Once the rail receptances are known, the corrugation model uses different modules to characterise the undulatory wear.

The railway vehicle dynamic simulation package DINATREN, developed by Santamaría [31], has been used to obtain the vehicle–rail contact parameters, including radii, forces and creepages.

The dynamic behaviour of the wheelset is analysed by means of the finite element method using the standard package MSC/NASTRAN [21]. The types of elements used are hex8, eight node hexahedron, and wedge6, triangular base prism.

In accordance with several authors (Frederick [32], Tassilly [2,3] and Hempelmann [6]), corrugation is explained, specifically for short wavelengths, as a complex feed-back process, which can be triggered by the presence of infinitesimal roughness on the running surface. This roughness induces an infinitesimal change of the variables defining the contact between wheel and rail, which is transferred, for each excitation frequency, to the vehicle and rail track dynamics. Their response will determine, through a wear mechanism, the wavelength, which increases the depth of the troughs of the original profile. This leads to an exponential corrugation development process governed by the real part of the exponent, known as function G. This function will be the indicator showing the most probable frequency for corrugation appearance.

The function G obtained for the inner wheel in the leading axle is shown in Fig. 8. According to function G, the corrugation process is likely to appear sooner at midspan around 200 Hz. Taking into account the vehicle

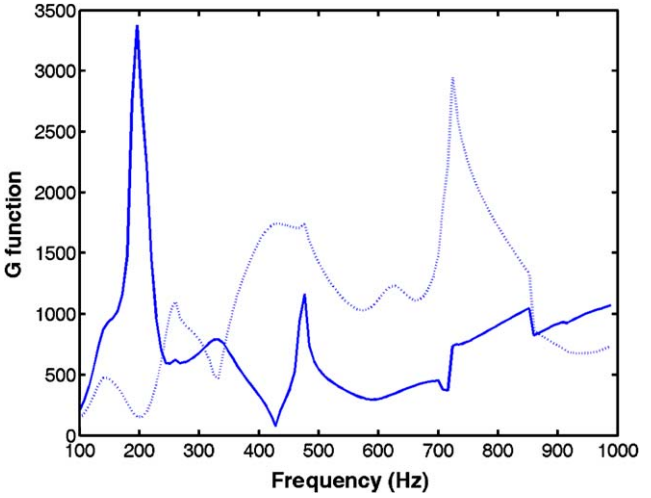

Fig. 8. G function showing the most probable frequency for corrugation appearance at midspan (-) and over sleeper (⋯).

velocity for this application case, $V = 13.4\,\mathrm{m/s}$, the corrugation wavelength predicted by the model provides a good match with experimental values.

On the basis of the linear model employed for the study of corrugation, and with the receptances obtained from the same point where corrugation was observed, it can be concluded that the phenomenon of undulatory wear, or corrugation, is provoked by the coincidence in frequency of the first lateral 'pinned–pinned' mode, where the head and the foot of the rail vibrate in anti-phase, and the mode where the sleeper vibrates independently, which produces an antiresonance in the vertical receptance.

8. Conclusions

This article presents a model to describe the dynamic behaviour of the track for both the vertical and the lateral component, taking into account the discrete nature of the support, using the FSM and the theory of periodic structures.

In order to contrast this model with a reference tool, the results obtained with the model for a finite section of track were compared with those given by the commercial finite element programme MSC/NASTRAN [21].

The differences observed after such comparison led to the inclusion in the track model of the modal truncation augmentation method [24,25] extended to wave superposition. This obtains greater accuracy of results.

The track model results were also compared to those obtained by the infinite track models developed by Gry [16] and Müller [7], always restricting for the model the capacities not taken into consideration by these two authors. As the article shows, comparison with these models was satisfactory.

The track model presented here, including all the abovementioned improvements, was used to study a case of corrugation on a specific track. The results obtained for receptances and for prediction of corrugation match the values obtained from experiments.

In the application case studied in Bilbao, since the distance between sleepers was 1 m, the studied frequency range was at low frequency. However, the track model developed in this paper is thought to be used in a general way to study problems of corrugation, independently of the frequency range where the phenomenon takes place. This would allow to study others cases largely examined in the literature [5,6,8,16], where typical distance between sleepers goes down to 0.6 m, and so that the corrugation study must be carried out at higher frequencies.

Acknowledgements

The authors are grateful to the Basque Government for its assistance through contract UE99/47.

References

[1] S.L. Grassie, J. Kalousek, Rail corrugation: characteristic, causes and treatments, *Proceedings of the Institution of Mechanical Engineers* 207 (1993) 57–68.
[2] E. Tassilly, N. Vincent, A linear model for the corrugation of rails, *Journal of Sound and Vibration* 150 (1) (1991) 25–45.
[3] E. Tassilly, N. Vincent, Rail corrugations: analytical model and field tests, *Wear* 144 (1991) 163–178.
[4] S.L. Grassie, R.W. Gregory, D. Harrison, K.L. Johnson, The dynamic response of railway track to high frequency vertical/lateral/longitudinal excitation, *Journal of Mechanical Engineering Science* 24 (1982) 77–102.
[5] B. Ripke, K. Knothe, Simulation of high frequency vehicle–track interactions, *Vehicle System Dynamics Supplement* 24 (1995) 72–85.
[6] K. Hempelmann, K. Knothe, An extended linear model for the prediction of short pitch corrugation, *Wear* 191 (1996) 161–169.
[7] S. Müller, A linear vehicle–rail model to investigate stability and corrugation on straight track, *Wear* 243 (2000) 122–132.
[8] K. Knothe, S.L. Grassie, Modelling of railway track and vehicle/track interaction at high frequencies, *Vehicle System Dynamics* 23 (1993) 209–262.
[9] K. Knothe, Z. Strzyzakowski, K. Willner, Rail vibrations in the high frequency range, *Journal of Sound and Vibration* 169 (1) (1994) 111–123.
[10] D.J. Thompson, Vehicle–rail noise generation, part III: rail vibration, *Journal of Sound and Vibration* 161 (1993) 421–446.
[11] T.X. Wu, D.J. Thompson, A double Timoshenko beam model for vertical vibration analysis of railway track at high frequencies, *Journal of Sound and Vibration* 224 (2) (1999) 329–348.
[12] T.X. Wu, D.J. Thompson, Analysis of lateral vibration behaviour of railway track at high frequencies using a continuously supported multiple beam model, *Journal of Acoustical Society of America* 106 (3) (1999) 1369–1373.
[13] T.X. Wu, D.J. Thompson, Vibration analysis of railway track with multiple wheels on the rail, *Journal of Sound and Vibration* 239 (1) (2001) 69–97.
[14] T.X. Wu, D.J. Thompson, An investigation into rail corrugation due to micro-slip under multiple wheel/rail interactions. *ISVR Technical Memorandum* No. 887. April 2002.
[15] L. Gavric, Computation of propagative waves in free rail using a finite element technique, *Journal of Sound and Vibration* 185 (3) (1995) 531–543.
[16] L. Gry, Dynamic modelling of railway track based on wave propagation, *Journal of Sound and Vibration* 195 (3) (1996) 477–505.
[17] L. Gry, C. Gontier, Dynamic modelling of railway track: a periodic model based on a generalised beam formulation, *Journal of Sound and Vibration* 199 (4) (1997) 531–558.
[18] D.J. Mead, Wave propagation and natural modes in periodic systems. Part I and II, *Journal of Sound and Vibration* 40 (1975) 1–39.
[19] (MATLAB 6 Release 12), *User's Manual*, The MathWorks, Inc., Natick, MA, 2001.
[20] MAPLE 7, *User's Manual*, Waterloo Maple Inc., Waterloo, Canada, 2001.
[21] MSC/NASTRAN Version 70.7, *User's Manual*, Mac Neal-Schwendler, MSC. Software, GmbH, Munich, Germany, 2002.
[22] Y.K. Cheung, *Finite Strip Method in Structural Analysis*, Pergamon Press, Oxford, 1976.
[23] MAPLE V Release 4, *User's Manual*, Waterloo Maple Inc., Waterloo, Canada, 1996.
[24] J.M. Dickens, J.M. Nakagaka, Wittbrodt: a critique of mode acceleration and modal truncation augmentation methods for modal response analysis, *Computers and Structures* 62 (6) (1997) 985–998.
[25] T. Rose, Using residual vectors in MSC/NASTRAN dynamic analysis to improve accuracy. Presented at the 1991 *MSC World Users' Conference*.
[26] E.G. Vadillo, J.A. Tárrago, G. Gárate, C. Angulo, Effect of sleeper distance on rail corrugation, *Wear* 217 (1998) 140–146.
[27] I. Gómez, E.G. Vadillo, An analytical approach to study a special case of booted sleeper track rail corrugation, *Wear* 251 (2001) 916–924.
[28] I. Gómez, E.G. Vadillo, A linear model to explain short pitch corrugation on rails, *Wear* 255 (2003) 1127–1142.
[29] R.A. Clark, G.A. Scott, W. Poole, Short wave corrugation—an explanation based on slip-stick vibrations, *Applied Mechanics Rail Transportation Symposium*, AMD Vol. 96, RTD Vol. 2, ASME, 1998, pp. 141–148.
[30] R.A. Clark, Rail corrugation—recent theories. in: *Track Technology*, Thomas Telford, London, 1985, pp. 89–115.
[31] J. Santamaría, DINATREN: una nueva herramienta para la simulación de vehículos ferroviarios (A new tool for simulation of rail vehicles), *Anales de Ingeniería Mecánica* (2000).
[32] C.O. Frederick, A rail corrugation theory, *Proceedings of the International Symposium Contact Mechanics and Wear of Rail/Wheel Systems II* (1986) 181–212.